ARTICLES

Ultrafast Photoinduced Electron Transfer within a Self-Assembled Donor−Acceptor System

Anouk Dirksen, Cornelis J. Kleverlaan,† Joost N. H. Reek, and Luisa De Cola*

HIMS, Universiteit van Amsterdam, Nieuwe Achtergracht 166, 1018 WV Amsterdam, The Netherlands

Received: January 12, 2005; In Final Form: April 17, 2005

A photoactive supramolecular assembly that is based on the hydrogen-bonded system **H1·G2**, consisting of a methyl viologen-functionalized barbiturate host **(H1)** (1-(*N*-(3,5-*bis*[[(6-*tert*-butylacetylamino-2-pyridyl)-amino]carbonyl])-phenylacetamide)-1′-methyl-4,4′-bipyridium) and a [Re(Br)$(CO)_3$(barbi-bpy)] (barbi-bpy = 5-[4-(4′-methyl)-2,2′-bipyridyl]methyl-2,4,6-(1*H*,3*H*,5*H*)-pyrimidinetrione) complex as the guest (**G2**) is described. The host molecule contains a well-known electron accepting group (methyl viologen), whereas the guest system can act as an efficient electron donor in the excited state. Upon self-assembly, the resulting adduct (**H1·G2**) represents an interesting noncovalently linked donor−acceptor system. The **H1·G2** complex has been characterized in acetonitrile-d_3 using ^{1}H NMR and diffusion-ordered NMR spectroscopy (DOSY). The photophysical properties of the components and of the assembly have been studied in dichloromethane, in which the assembly has a high binding constant ($K_{ass} \geq 2 \times 10^5$ M^{-1}), using time-resolved fluorescence and transient absorption spectroscopy. A detailed investigation of the hydrogen-bonded complex **H1·G2** revealed that, upon excitation of the rhenium compound **G2**, an ultrafast electron-transfer process occurs from the metal-based component to the acceptor unit. The kinetics of the forward and back electron-transfer processes have been determined.

Introduction

The assembly of smaller building blocks into more complicated systems using noncovalent interactions, such as hydrogen bonds and ionic and hydrophobic interactions, is still an emerging field in modern chemistry.[1−9] The supramolecular approach offers an elegant way to facilitate the synthesis of complicate structures, introducing new functions not present in the separate components, that could lead to the construction of molecular devices.[10] Molecular recognition is based on these interactions, enabling the selective assembly of host and guest molecules in a predefined way, which can be applied for the detection of specific molecules or ions in solution or for the construction of very large nanostructures.[11−16]

Among the processes that could emerge from the assembly of photoactive components, electron transfer certainly is of great interest. Several supramolecular assemblies have been synthesized and studied[17−23] to gain more insight in photoinduced electron transfer (PET) in noncovalently linked systems. The understanding of such processes and, in particular, the role played by the "connector" in the donor−acceptor assembly is extremely relevant, because it would contribute to a greater insight in the electron-transfer processes occurring in natural systems. In particular, hydrogen bonding has been applied to create a variety of electron donor−electron acceptor (D−A) dyads to study PET.[24−32] In these studies, the efficiency of the electron transfer was observed to be strongly dependent on several factors, such as distance, configuration, linker orientation, and directionality. It has been demonstrated that the rates of electron transfer processes in hydrogen-bonded D−A assemblies can be very similar to those of analogous covalently linked systems. However, so far, none of these systems enabled the creation of long-lived charge-separated states and long-range electron-transfer processes, i.e., a highly efficient and fast forward-electron transfer combined with a back-electron transfer process that is several orders of magnitude slower.

In this paper, we report the synthesis and photophysical properties of a dyad system in which the electron donor D and the electron acceptor A are assembled via hydrogen bonds. We demonstrate that ultrafast electron transfer processes can occur within the assembly and that the rate of the back-electron transfer is several orders of magnitude slower than the forward process.

The system was designed to have (i) a very high association constant for the host−guest components, to avoid any bimolecular process; (ii) a good D−A pair to have an exoergonic PET also in apolar solvents; (iii) significantly different absorption properties for the host and the guest to allow selective excitation; (iv) a donor with an emissive, long-lived excited state, to monitor the electron-transfer processes by emission spectroscopy; and (v) a radical anion and cation, formed as a result of PET with spectral features that can be detected by absorption transient spectroscopy.

The host, 1-(*N*-(3,5-*bis*[[(6-*tert*-butylacetylamino-2-pyridyl)-amino]carbonyl])-phenylacetamide)-1′-methyl-4,4′-bipyridium (**H1**) is based on a barbiturate receptor, which was reported, for the first time, in 1988 by Hamilton et al.,[33] with an appended viologen unit (electron acceptor). The guest (**G2**) is a barbiturate

† Current address: Department of Dental Materials Science, Academic Center for Dentistry Amsterdam (ACTA), Louwesweg 1, 1066 EA Amsterdam, The Netherlands.

10.1021/jp050207k CCC: $30.25
Published on Web 05/25/2005

SCHEME 1: Schematic Representation of the Components H1 and G2 and Their Host−Guest Complex H1·G2

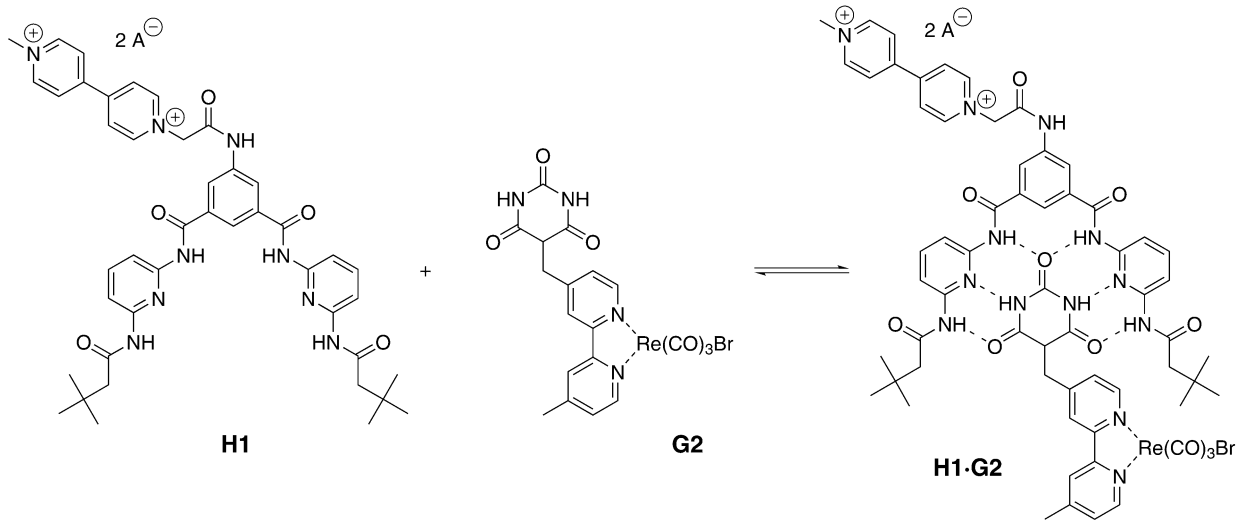

A = Br/I, PF_6, and BAr_f , where BAr_f is $\{B[3,5\text{-}(CF_3)_2C_6H_3]_4\}^-$.

derivative that is comprised of a luminescent rhenium complex (electron donor), $[Re(Br)(CO)_3$(barbi-bpy), where barbi-bpy = 5-[4-(4′-methyl)-2,2′-bipyridyl]methyl-2,4,6-(1*H*,3*H*,5*H*)-pyrimidinetrione (Scheme 1).

The host and guest motif were chosen because of the high association constant of the assembly (typically on the order of 10^5-10^8 M^{-1} in chlorinated solvents), which can be optimized using different substituents.[34] Furthermore, the complementarity of the host and the guest results in a 1:1 self-assembled complex, avoiding a statistic distribution of species in solution. The noncovalent linked dyad resulting from the self-assembly of **H1** and **G2** can be compared with the analogous covalent system having a rhenium complex that contains a bipyridine functionalized with a methyl viologen unit.[35−37]

The choice of the uncharged rhenium complex versus those that are most widely used in electron and energy transfer processes, $[Ru(bpy)_3]$ and $[Os(bpy)_3]$ derivatives,[38−43] was dictated by its solubility in chlorinated solvents in which the assembly is highly favorable. Nevertheless, rhenium compounds have been used as electron donors in combination with suitable electron acceptors, such as quinones and viologens.[35−37,44−49]

The self-assembly process was studied with nuclear magnetic resonance (NMR) spectroscopy. Association constants have been determined, and the photophysical properties of the separate components and of the assembly are reported. An efficient and ultrafast electron-transfer process within the host−guest complex **H1·G2** was observed, reflecting a similar kinetic profile as the covalently linked system that contained the same electron donor and acceptor units.

Experimental Section

Solvents and Starting Materials. All reagents used were obtained from available commercial sources and used without additional purification unless otherwise indicated. CH_2Cl_2 was distilled from CaH_2 and, tetrahydrofuran (THF) was distilled from Na/benzophenone. Commercial deuterated solvents were used as received for the characterization of the compounds. Acetonitrile-d_3 was distilled from CaH_2 and passed through 4-Å molecular sieves prior to use for the binding study.

Instrumentation. ^1H NMR and ^{13}C NMR spectra were recorded on a Varian model Inova500 system at 499.86 and 125.70 MHz, respectively. Diffusion measurements were performed on a Varian model Inova500 system equipped with a Performa II pulsed-gradient unit that was able to produce magnetic-field pulse gradients of ∼30 G/cm in the *z*-direction. The DOSY experiments were conducted in a 5-mm inverse probe at 295 K. The magnetic-field pulse gradients had a duration of 1 ms, followed by a stabilization time of 2 ms. The diffusion delay was set to 0.1 s. The magnetic-field pulse gradients were incremented from 0 G/cm to 25 G/cm in 10 steps, and the stimulated spin−echo experiment was performed with compensation for convection. The pulse sequence was developed by Evans and Morris (University of Manchester).[50] Fast atom bombardment mass spectrometry (FAB-MS) was performed using a JEOL model JMS SX/SX 102A four-sector mass spectrometer that was coupled to a JEOL MS-MP9021D/UPD system program. Samples were loaded in a matrix solution (3-nitrobenzyl alcohol) onto a stainless-steel probe and bombarded with Xe atoms with an energy of 3 keV. During the high-resolution FAB-MS measurements, a resolving power of 10 000 (10% valley definition) was used. UV−Vis absorption spectra were recorded on a diode-array Hewlett−Packard model HP8453 spectrophotometer at 293 K. Fluorescence spectra were recorded on a SPEX fluorometer. Full transient absorption spectra were obtained 10 ns after the laser pulse (1 frame, 50 accumulations, 4 mJ/pulse) that was excited with a 2-ns (full width at half maximum, fwhm) Coherent YAG laser (repetition rate of 10 Hz) at 435 nm and using an OMA detection system. Nanosecond flash photolysis emission kinetics was measured by irradiating the sample at 435 nm with a 2-ns (fwhm) Coherent Infinity XPO laser (repetition rate of 10 Hz). In the case of the nanosecond flash transient kinetics, a pulsed xenon lamp perpendicular to the laser beam was used as a probe light. The 450-W xenon lamp was equipped with a Müller Electronik MSP05 pulsing unit giving pulses of 0.5 ms. The light was collected in an Oriel monochromator, detected by a P28 PMT (Hamamatsu), and recorded on a Textronic TDS3052 (500 MHz) oscilloscope. The laser oscillator, Q-switch, lamp, shutter and trigger were externally controlled with a homemade digital logic circuit, which allowed synchronous timing. The absorption transients were plotted as $\Delta A = \log(I_0/I_t)$ versus time, where I_0 was the monitoring light intensity prior the laser pulse and I_t the observed signal at delay time *t*. The femtosecond transient absorption (TA) setup used to probe the processes that are occurring within 1 ns has been described previously.[51] The optical density of the sample solutions was in the range of 0.5−

1.0 at the wavelength of excitation. The output of the laser was ~2 μJ/pulse.

Determination of the Association Constant (K_{ass}) of PF_6^-·H1·G2 in Acetonitrile-d_3. The association constant of PF_6^-·**H1**·**G2** in acetonitrile-d_3 was calculated from the ratio between the free components and the assembly, which was determined from the integrals of their proton signals. Because the ratio between the free components and the complex is dependent on the concentration, solutions that contain 5 mM, 2.5 mM, and 1.0 mM PF_6^-·**H1** and **G2** have been measured subsequently to obtain an accurate value for K_{ass}.

Determination of the Association Constant (K_{ass}) of BAr_f^-·H1·G2 in CH_2Cl_2. Time-resolved fluorescence measurements were performed for a solution that contains 5×10^{-4} M BAr_f^-·**H1**·**G2** to determine the association constant in CH_2Cl_2. The association constant was calculated from the amount of **G2** emission quenched in the presence of 1 equiv of BAr_f^-·**H1**, assuming that the electron transfer from **G2** to the methyl viologen moiety is 100% efficient.

Preparation of the Methyl Viologen-Functionalized Barbiturate Receptor. 1-Methyl-4,4′-bipyridinium (iodide) was prepared according to a literature procedure.[52]

3,5-*Bis*[[(6-*tert*-butylacetylamino-2-pyridyl)amino]carbonyl]-aniline (1). 1 was prepared according to literature procedures.[53−55]

2-Bromo-*N*-(3,5-*bis*[[(6-*tert*-butylacetylamino-2-pyridyl)-amino]carbonyl])-phenylacetamide (2). A solution of **1** (0.49 g, 0.88 mmol) and 4-(dimethylamino)pyridine (50 mg, 0.41 mmol) in 20 mL of dry THF was added dropwise to a solution of bromoacetyl chloride (234 mg, 1.32 mmol) in 10 mL of dry THF cooled at 0 °C, under vigorous stirring. After 2 h, the reaction mixture was quenched with H_2O and extracted with 3 × 30 mL of CH_2Cl_2. The organic extract was washed with 3 × 10 mL of a saturated $NaHCO_3$ solution, dried with anhydrous $MgSO_4$, and concentrated under reduced pressure, yielding 0.53 g of **5** (0.78 mmol, 88.6%) as a white solid. ^{1}H NMR (DMSO-d_6): δ (ppm) = 1.02 (s, C(CH_3)$_3$), 2.31 (s, CH_2C(CH$_3$)$_3$), 4.11 (s, CH_2Br), 7.80 (m, H_{py}-3, H_{py}-4, H_{py}-5), 8.28 (s, H_{ar}-4), 8.35 (s, H_{ar}-2, H_{ar}-6), 10.00 (s, two C_{py}CONH), 10.42 (s, two C_{ar}CONH), 10.82 (s, C_{ar}CONH). ^{13}C NMR (DMSO-d_6): δ (ppm) = 29.6, 30.2, 30.9, 49.1, 110.1, 110.4, 121.9, 122.3, 134.9, 139.1, 140.1, 150.0, 150.5, 165.0, 165.4, 170.9. HRMS (FAB) Calcd. for $C_{32}H_{39}N_7O_5{}^{79}Br$ (MH^+): 680.2196. Found: 680.2141. HRMS (FAB) Calcd. for $C_{32}H_{39}N_7O_5{}^{81}Br$ (MH^+): 682.2182. Found: 682.2155.

1-(*N*-(3,5-Bis[[(6-*tert*-butylacetylamino-2-pyridyl)amino]-carbonyl])-phenylacetamide)-1′methyl-4,4′-bipyridium (Br^-/I^-) (X−H1). 1-Methyl-4,4′-bipyridium (iodide) (184 mg, 0.619 mmol) was refluxed overnight with 1 equiv of **2** (420 mg, 0.617 mmol) in acetonitrile. The halide salt was filtered from the cooled solution and washed with a small amount of acetonitrile, yielding 0.38 g of X−**H1** (0.388 mmol, 62.6%) as a red-brownish powder. ^{1}H NMR (DMSO-d_6): δ (ppm) = 1.01 (s, C(CH_3)$_3$), 2.30 (s, CH_2C(CH$_3$)$_3$), 4.46 (s, bpy-CH_3), 5.87 (s, bpy-CH_2), 7.79 (m, H_{py}-4), 7.84 (m, H_{py}-3, H_{py}-5), 8.33 (s, H_{ar}-4), 8.37 (s, H_{ar}-2, H_{ar}-6), 8.82 (d, J = 5.50 Hz, H_{bpy}-3′, H_{bpy}-5′), 8.90 (d, J = 5.50 Hz, H_{bpy}-2′, H_{bpy}-6′), 9.34 (d, J = 5.50 Hz, H_{bpy}-3, H_{bpy}-5), 9.40 (d, J = 5.50 Hz, H_{bpy}-2, H_{bpy}-6), 9.98 (s, two C_{py}CONH), 10.46 (s, two C_{ar}CONH), 11.41 (s, C_{ar}CONH). ^{13}C NMR (DMSO-d_6): δ (ppm) = 29.6, 30.9, 48.1, 49.1, 62.2, 110.1, 110.4, 122.0, 122.5, 126.1, 126.3, 134.9, 138.8, 140.2, 146.7, 147.5, 148.1, 149.4, 150.0, 150.5, 163.7, 164.9, 171.0. HRMS (FAB) calcd. for $C_{43}H_{49}N_9O_5{}^{79}Br$ (MH^+-I^-), 852.3030. Found: 852.3044. HRMS (FAB) calcd. for $C_{43}H_{49}N_9O_5{}^{81}Br$ (MH^+-I^-), 850.3040. Found: 850.3055.

1-(*N*-(3,5-bis[[(6-*tert*-butylacetylamino-2-pyridyl)amino]-carbonyl])-phenylacetamide)-1′-methyl-4,4′-bipyridium ($2PF_6^-$) (PF_6^-−H1). X−**H1** (0.38 g, 0.388 mmol) was dissolved in water and then precipitated by adding a concentrated solution of NH_4PF_6 in water to yield 296 mg (0.276 mmol, 72.6%) of PF_6^-−**H1**: ^{1}H NMR (acetonitrile-d_3): δ (ppm) = 1.05 (s, C(CH_3)$_3$), 2.26 (s, CH_2C(CH$_3$)$_3$), 4.42 (s, bpy-CH_3), 5.58 (s, bpy-CH_2), 7.85 (m, H_{py}-3, H_{py}-4, H_{py}-5), 8.13 (s, H_{ar}-4), 8.26 (s, H_{ar}-2, H_{ar}-6), 8.42 (d, J = 7.00 Hz, H_{bpy}-3′, H_{bpy}-5′), 8.47 (d, J = 7.00 Hz, H_{bpy}-2′, H_{bpy}-6′), 8.55 (s, two C_{py}CONH), 8.87 (d, J = 7.00 Hz, H_{bpy}-3, H_{bpy}-5), 8.92 (d, J = 7.00 Hz, H_{bpy}-2, H_{bpy}-6), 9.09 (s, two C_{ar}CONH), 9.26 (s, C_{ar}CONH). ^{13}C NMR (DMSO-d_6): δ (ppm) = 29.9, 31.8, 49.7, 50.8, 63.5, 110.6, 110.7, 123.1, 123.4, 127.7, 128.0, 136.6, 139.4, 141.6, 147.5, 148.3, 150.6, 150.9, 151.4, 152.0, 163.6, 165.7, 172.1. HRMS (FAB) calcd. for $C_{43}H_{49}N_9O_5PF_6$ ($MH^+-PF_6^-$): 916.3498. Found: 916.3452.

Na{B[3,5-(CF$_3$)$_2$C$_6$H$_3$]$_4$} (NaBAr$_f$). Na{B[3,5-(CF$_3$)$_2$C$_6$H$_3$]$_4$} ($NaBAr_f$) has been prepared according to a literature procedure.[56]

1-(*N*-(3,5-bis[[(6-*tert*-butylacetylamino-2-pyridyl)amino]-carbonyl])-phenylacetamide)-1′-methyl-4,4′-bipyridium ($2BAr_f^-$) (Bar_f-H1). X−**H1** (256.5 mg, 0.262 mmol) was dissolved in water and extracted with diethyl ether containing 1.8 equivalents of $NaBAr_f$ (440.7 mg, 0.50 mmol). The diethyl ether layer was collected and the solvent was removed in vacuo to yield 0.56 g (0.224 mmol, 89.7%) of Bar_f-**H1**: ^{1}H NMR (DMSO-d_6): δ (ppm) = 1.01 (s, C(CH_3)$_3$), 2.29 (s, CH_2C-(CH$_3$)$_3$), 4.46 (s, bpy-CH_3), 5.81 (s, bpy-CH_2), 7.83 (m, H_{py}-3, H_{py}-4, H_{py}-5), 8.33 (s, H_{ar}-4), 8.37 (s, H_{ar}-2, H_{ar}-6), 8.80 (d, J = 7.00 Hz, H_{bpy}-3′, H_{bpy}-5′), 8.88 (d, J = 7.00 Hz, H_{bpy}-2′, H_{bpy}-6′), 9.32 (d, J = 7.00 Hz, H_{bpy}-3, H_{bpy}-5), 9.36 (d, J = 7.00 Hz, H_{bpy}-2, H_{bpy}-6), 9.95 (s, two C_{py}CONH), 10.45 (s, two C_{ar}CONH), 11.20 (s, C_{ar}CONH). ^{13}C NMR (DMSO-d_6): δ (ppm) = 29.5, 29.5, 30.8, 48.1, 49.1, 110.2, 110.3, 117.6 (septet, $^3J(^{13}C,^{19}F)$ = 3.77 Hz), 122.0, 124.0 (q, $^1J(^{13}C,^{19}F)$ = 271.5 Hz), 126.3, 127.2, 128.5 (m, $^4J(^{13}C,^{11}B)$ = 2.9 Hz, $^2J(^{13}C,^{19}F)$ = 31.8 Hz), 134.0, 135.0, 138.7, 140.1, 146.7, 147.5, 148.2, 149.5, 149.9, 150.5, 161.0 (q, $^2J(^{13}C,^{11}B)$ = 49.7 Hz), 161.0 (t, $^2J(^{13}C,^{10}B)$ = 50.3 Hz), 163.6, 164.8, 170.9. HRMS (FAB) calcd. for $C_{107}H_{74}N_9O_5B_2F_{48}$ (MH^+): 2497.5262. Found: 2498.5107. UV−Vis λ_{max} (ϵ in M^{-1} cm^{-1}) (CH_2Cl_2): 302 nm (34000).

Barbituric Acid-Functionalized Bipyridine Ligand. 5-[4-(4′-Methyl)-2,2′-bipyridyl]methyl-2,4,6-(1*H*,3*H*,5*H*)-pyrimidinetrione (barbi-bpy) was prepared according to a literature procedure.[57]

Preparation of the Rhenium Complex: [Re(Br)(CO)$_3$-(barbi-bpy)] (G2). A solution of [Re(Br)(CO)$_5$] (0.41 g, 1.01 mmol) and (barbi-bpy) (0.29 g, 0.93 mmol) in 50 mL of acetonitrile was heated at reflux under N_2 overnight. After the evaporation of acetonitrile and washing with pentane, ether, and dichloromethane (DCM), 0.34 g (55.4%, 0.52 mmol) of **G2** was obtained as a yellow powder: ^{1}H NMR (acetonitrile-d_3): δ (ppm) = 2.57 (s, bpy-4′-CH_3), 3.50 (d, J = 5.0 Hz, CH_2), 4.07 (t, J = 5.0 Hz, CH), 7.45 (d, J = 5.5 Hz, H_{bpy}-5′), 7.48 (d, J = 5.5 Hz, H_{bpy}-5), 8.27 (s, H_{bpy}-3′), 8.32 (s, H_{bpy}-3), 8.84 (d, J = 5.5 Hz, H_{bpy}-6′), 8.87 (d, J = 5.5 Hz, H_{bpy}-6), 9.02 (2 × s, two NH). ^{13}C NMR (acetonitrile-d_3): δ (ppm) = 21.6, 32.3, 49.8, 125.6, 125.7, 126.6, 126.7, 128.9, 129.2, 153.5, 153.6, 156.2, 156.5, 169.1, 172.5, 190.5, 198.5. IR (CH_2Cl_2): ν(C=O) 2033 cm^{-1} (s), 2023 cm^{-1} (s), 1918 cm^{-1} (s). HRMS (FAB) calcd.

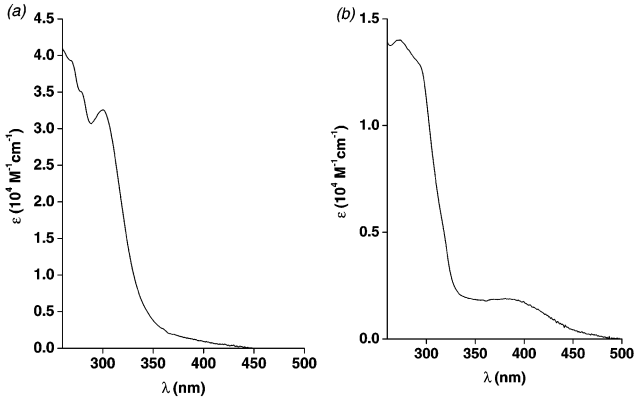

Figure 1. Absorption spectra of (a) BAr_f−**H1** and (b) **G2** in CH_2Cl_2.

for $C_{19}H_{14}O_6N_4{}^{79}BrRe$ (MH^+): 659.9637, found 659.9659. UV−Vis λ_{max} (ϵ in $M^{-1}cm^{-1}$) (CH_2Cl_2): 372 nm (1900).

Results and Discussion

Synthesis and Characterization of Guest and Host Molecules. The host−guest system described in this paper is based on a barbiturate receptor, which forms a very strong host−guest complex, based on six hydrogen bonds with barbiturate and its derivatives. The barbiturate receptor was functionalized with a methyl viologen unit, which is a well-known electron acceptor moiety (Scheme 2). Compound **1**, which was prepared according to literature procedures,[53−55] was functionalized by reaction with bromoacetyl chloride to give **2**. Subsequent alkylation of **2** with a methyl viologen group rendered **H1**.

H1 was obtained as a halide salt, X−**H1**, and the halides were exchanged for PF_6^- by precipitation from water when a concentrated solution of NH_4PF_6 in water was added, giving PF_6−**H1**, which is soluble in acetonitrile. Furthermore, the halides were also exchanged for $\{B[3,5\text{-}(CF_3)_2C_6H_3]_4\}^-$ (BAr_f^-) via extraction of X−**H1** from the aqueous layer to a diethyl ether layer containing 1.8 equiv of $NaBAr_f$, giving BAr_f−**H1**, which is soluble in apolar solvents such as DCM.

[Re(Br)(CO)$_3$(barbi-bpy)] was used as a guest molecule and synthesized by refluxing [Re(Br)(CO)$_5$] with the barbituric acid-functionalized bipyridine ligand[57] (barbi-bpy) in acetonitrile. Subsequent extensive washing with DCM and pentane yielded the desired guest [Re(Br)(CO)$_3$(barbi-bpy)] (**G2**).

All compounds were characterized using ^{1}H NMR, ^{13}C NMR, and high-resolution FAB-MS. In addition, ground-state UV−Vis absorption and emission spectra were recorded for both BAr_f−**H1** and **G2** in DCM.

Photophysical Properties of BAr_f−H1 and G2. The ground-state UV−Vis absorption spectrum in DCM of BAr_f−**H1** shows an absorption maximum at 302 nm (ϵ = 34 000 M^{-1} cm^{-1}) (Figure 1a) assigned to $\pi-\pi^*$ transitions, which is in good agreement with the absorption at 304 nm reported by Hamilton et al.[53] for a barbiturate receptor.

The photophysical properties of **G2** are very similar to those reported for [Re(Br)(CO)$_3$(bpy)].[58] The UV−Vis absorption spectrum shows, in the high-energy region, the bpys $\pi-\pi$ transitions and at lower energy, the characteristic metal-to-ligand charge transfer (^{1}MLCT) Re → bpy, absorption band at 372 nm (ϵ = 1900 M^{-1} cm^{-1}) (see Figure 1b). The emission that occurs from the ^{3}MLCT state has a maximum at 590 nm with an excited-state lifetime of 60 ns in DCM.

Characterization of PF_6−H1·G2 in Acetonitrile-d_3 by ^{1}H NMR. The assembly PF_6−**H1·G2** was studied using ^{1}H NMR techniques to gain more insight in the structure of the host−guest complex in solution. Unfortunately, the solubility of **G2** was insufficient in chlorinated solvents to conduct an accurate NMR titration. However, in acetonitrile-d_3, the solubility and the binding constant were determined to be sufficient high to characterize the PF_6−**H1·G2** assembly. When PF_6−**H1** was added to **G2**, three sets of proton signals appeared: one set that originated from free PF_6−**H1**, one that originated from free **G2**, and one that originated from the assembly PF_6−**H1·G2**. The aromatic region of the free components (PF_6−**H1** and **G2**) and of the host−guest complex (PF_6−**H1·G2**) are displayed in Figure 2.

The appearance of distinct signals shows that the exchange between the free components and the host−guest complex is slow on a NMR time scale. The formation of the assembly PF_6−**H1·G2** is evident from the clear shift of the proton signals, from 7.52 and 7.51 ppm in free **G2** to 7.58 and 7.41 ppm in PF_6−**H1·G2**, originating from H-5,5′ of the bipyridine ligand. From the ratio between the integrals of the bipyridine signals corresponding to free **G2** and those corresponding to the PF_6−**H1·G2** adduct at different concentrations, the binding constant in acetonitrile-d_3 was calculated to be 4.3 × 10^2 M^{-1}.

Diffusion-Ordered NMR Spectroscopy (DOSY). DOSY is a NMR technique that has been proven to be valuable for the characterization of supramolecular complexes. Mixtures of compounds can be analyzed by separation of their signals based on the difference in diffusion coefficients and consequently information about the hydrodynamic radius of molecules or assemblies in solution can be obtained.[59,60] The formation of a host−guest complex can result in a significant decrease in the diffusion coefficient of the components and can be probed with DOSY.

A DOSY experiment was performed for an equimolar (2.5 mM) solution of PF_6−**H1** and **G2** in acetonitrile-d_3. At these concentrations, the free components as well as the host−guest

SCHEME 2: Synthesis of X−H1 Starting from the Amine-Functionalized Receptor (1)

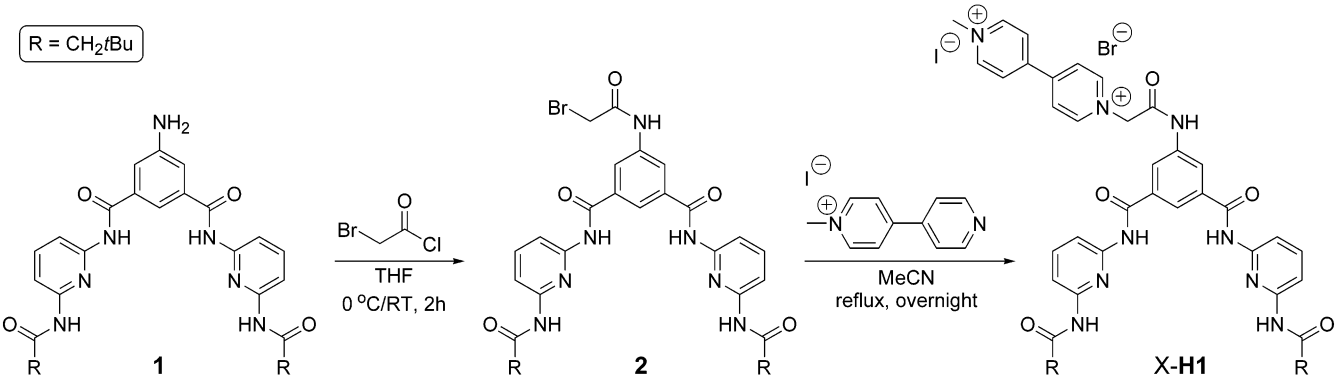

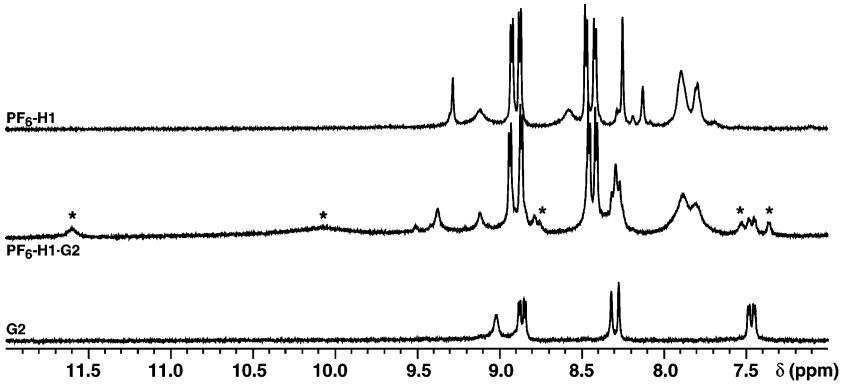

Figure 2. ^{1}H NMR spectra (aromatic region) of PF_6−**H1**, **G2**, and PF_6−**H1·G2** (2.5 mM in acetonitrile-d_3); characteristic signals of the host−guest complex PF_6−**H1·G2** are marked with an asterisk (*).

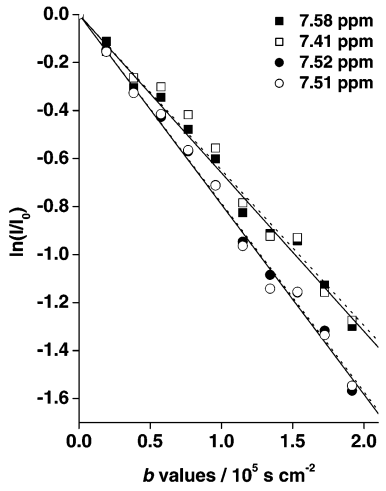

Figure 3. A Stejskal-Tanner plot[61,62] of the experimental peak areas of the proton signals corresponding to bpy-H5,5′ of free **G2** (7.51 and 7.52 ppm) and of bound **G2** (7.41 and 7.58 ppm). Solid lines represent linear least-squares fits to the data ($R > 0.99$); b values are determined using $b = \gamma^2\delta^2G^2(\Delta - \delta/3)$; the slope of the line is equal to $-D$.

TABLE 1: Diffusion Coefficients (D_{exp}) Determined Using DOSY and the Experimental Hydrodynamic Radii (r_{exp}) of PF_6−H1, G2, and PF_6−H1·G2

D_{exp} ($\times 10^{-9}$ m^2/s)	r_{exp} (Å)
PF_6−**H1**	
0.55 ± 0.02^a	10.9 ± 0.4^a
0.59 ± 0.03^b	10.1 ± 0.5^b
G2	
0.65 ± 0.03^c	9.2 ± 0.4^c
0.79 ± 0.03^a	7.6 ± 0.3^a
PF_6−**H1·G2**	
0.86 ± 0.03^b	7.0 ± 0.3^b
0.64 ± 0.04^a	9.3 ± 0.6^a

[a] Determined from the mixture ($c = 2.5$ mM for both components). [b] Determined from a pure solution (at $c = 2.5$ mM). [c] Determined from a pure solution (at $c = 0.1$ mM).

complex are present in sufficient amounts for detection by NMR. A Stejskal−Tanner plot[61,62] of the H5,5′-bpy signals of free **G2** and of the host−guest complex PF_6−**H1·G2** shows that the assembly PF_6−**H1·G2** has a lower diffusion coefficient, as compared to free **G2** (Figure 3 and Table 1). In a similar fashion, the diffusion coefficient of free PF_6−**H1** could be determined from the ^{1}H NMR signals of the viologen unit (see Table 1). For comparison, the diffusion coefficients of PF_6−**H1** and **G2** in their free monomeric form were determined in separate DOSY experiments (see Table 1). These were determined to be in good agreement with the diffusion coefficients of the free components in the mixture. Using the Stokes−Einstein equation,[63] the hydrodynamic radius (r_{exp}) of each component could be calculated (see Table 1).

As expected, the hydrodynamic radius of PF_6−**H1·G2** was larger than that of free **G2**. Surprisingly, the hydrodynamic radius of the assembly PF_6−**H1·G2** (9.3 Å) was determined to be smaller than that of free PF_6−**H1** (10.9 Å), suggesting that PF_6−**H1** forms aggregates at a concentration of 2.5 mM. Indeed, a dilution study of PF_6−**H1** using ^{1}H NMR spectroscopy revealed that PF_6−**H1** self-aggregates at the concentration of 2.5 mM. A broadening of the aromatic signals of the pyridine rings and a shift in the signals corresponding to the NH groups within the binding motive are observed at concentrations of >0.5 mM. In addition, from a DOSY experiment measured at a concentration of 0.1 mM, a smaller hydrodynamic radius (9.2 Å) was calculated for PF_6−**H1** (see Table 1). The reduction of the hydrodynamic radius going from free PF_6−**H1** (10.9 Å) to the host−guest complex PF_6−**H1·G2** (9.3 Å) indicates that the aggregates of self-associated PF_6−**H1**, which exist at a concentration of 2.5 mM, dissociate upon binding to **G2**.

Photophysical Study for BAr_f-H1·G2. The photophysical properties of the assembly BAr_f−**H1·G2** were studied in DCM. A high binding constant in DCM, which is anticipated to be on the order of 10^5 M^{-1},[33,34] enables to study the photoinduced processes at low concentrations, while bimolecular processes between the two free components are prevented.

The measurements for the separate components BAr_f−**H1** and **G2**, and, for the assembly, BAr_f−**H1·G2** were performed at a concentration of 5×10^{-4} M. At this concentration, because of the relatively short-lived excited state (60 ns) of the donor system (**G2**), bimolecular quenching processes are negligible. In any case, a control experiment was performed in which a reference system was used consisting of a 5×10^{-4} M solution of an unsubstituted dimethyl viologen with 1 equivt of **G2** in acetonitrile. Excitation of this sample with 435-nm laser light (with an energy of 4 mJ/pulse) did not result in the quenching of the excited state of **G2**.

As mentioned previously, the rhenium complex **G2** has a characteristic ^{3}MLCT emission with a maximum at 590 nm (Figure 4a). Steady-state emission measurements indicated a strong reduction of the emission quantum yield when 1 equiv of the host molecule, BAr_f−**H1**, was added, although a very weak emission was observed for the BAr_f−**H1** component. The true nature of this emission was not further investigated. To calculate quantitatively the decrease in emission intensity of the metal-based component and to determine the rate of the process causing the quenching, time-resolved emission measurements

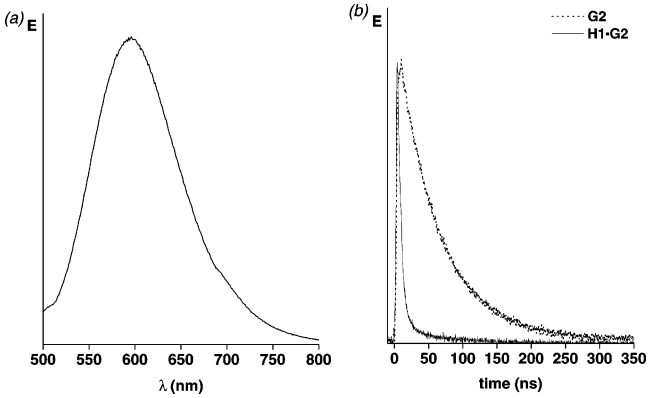

Figure 4. (a) Emission spectrum of **G2** in CH_2Cl_2 and (b) the emission decay of **G2** and of the host−guest complex BAr_f−**H1·G2** probed at 600 nm (CH_2Cl_2; $\lambda_{exc} = 435$ nm).

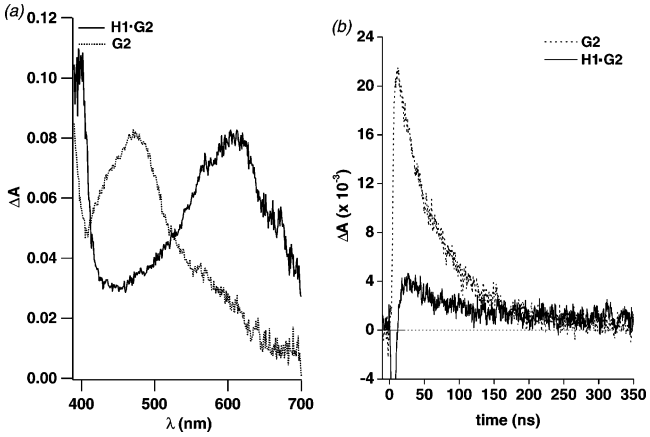

Figure 5. (a) Full transient absorption (TA) spectrum of **G2** and of the host−guest complex BAr_f−**H1·G2** recorded 10 ns after the laser pulse (CH_2Cl_2; $\lambda_{exc} = 435$ nm; 50 accumulations) and (b) the transient absorption trace probed at 470 nm for **G2** and BAr_f−**H1·G2** (CH_2Cl_2; $\lambda_{exc} = 435$ nm).

were performed. Traces of the decay of the luminescent excited state of **G2** have been recorded at $\lambda_{probe} = 600$ nm in the absence (and in the presence) of BAr_f−**H1**. Both traces are compared in Figure 4b.

From the emission decay at 600 nm, the lifetime of the ^{3}MLCT state of **G2**, in the absence of the receptor, was determined to be 60 ns. The addition of 1 equiv of BAr_f−**H1** resulted in a quenching of the **G2** excited state of >90%. The lifetime of the ^{3}MLCT excited state of **G2** in BAr_f−**H1·G2** is reduced to <3 ns (below the time resolution of our nanosecond equipment). Assuming that the quenching of the excited state of **G2** in the host−guest complex BAr_f−**H1·G2** is 100% efficient, the binding constant was calculated to be $\geq 2 \times 10^5$ M^{-1} in DCM.

The quenching process that takes place when excitation of the rhenium moiety occurs can easily be ascribed to a photoinduced electron transfer from the metal-based unit to the electron acceptor moiety containing the viologen. The photoinduced process is exoergonic with a ΔG value of −0.43 eV, as estimated from the electrochemical potential of the separate components[37b] and the E^{00} value of the rhenium component (2.1 eV, calculated by the low-temperature emission maximum). To gain more insight into the true nature of the photophysical processes that occur between BAr_f−**H1** and **G2** in the host−guest complex BAr_f−**H1·G2** and to calculate the rates of the processes, TA spectroscopy was performed. Figure 5a shows the nanosecond transient absorption spectrum of **G2** after

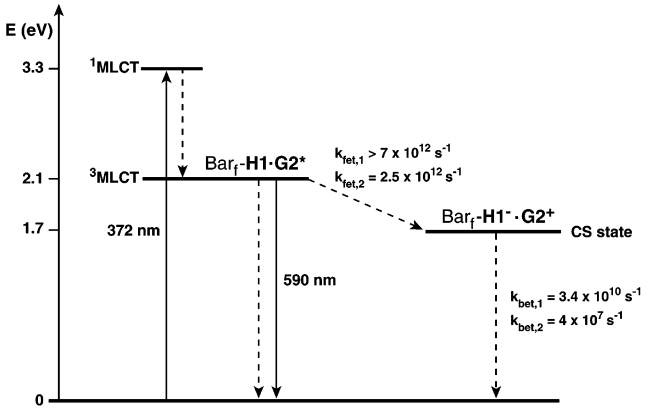

Figure 6. Schematic energy diagram showing the main processes occurring in the BAr_f−**H1·G2** assembly upon excitation of the **G2** component.

excitation at 435 nm, 10 ns after the laser pulse. The spectral properties of **G2** with the characteristic absorption at 470 nm of the ^{3}MLCT excited state are similar to those previously reported for $[Re(Br)(CO)_3(bpy)]$.[58] After the addition of 1 equiv of BAr_f−**H1**, new absorption bands are formed with maxima at 400 and 610 nm, respectively (see Figure 5a). By comparison with the TA spectrum of reduced viologen,[64] the new signals can be assigned to the radical anion of the methyl viologen moiety attached to the receptor.

Because free BAr_f−**H1** does not give any TA after excitation at 435 nm, excitation in the MLCT band of **G2** in the assembly results indeed in a photoinduced electron transfer from the excited metal complex to the methyl viologen moiety attached to the receptor within the laser pulse (2 ns fwhm). The ^{3}MLCT excited state of **G2** is strongly quenched after the addition of BAr_f−**H1** (see Figure 5b), resulting in the almost-quantitative disappearance of the TA signal of the ^{3}MLCT excited state of the rhenium complex at 470 nm and the formation of the viologen radical anion (see Figure 5a). The main processes that occur within the assembly after light excitation are summarized in the energy diagram that is shown in Figure 6.

To investigate the back-electron transfer process in BAr_f−**H1·G2**, TA traces were recorded probing at 400 and 610 nm, which are the absorption maxima of the reduced methyl viologen moiety. The recovery from the charge-separated (CS) state to the ground state shows double exponential kinetics on a nanosecond time scale (Figure 7).

The TA trace ($\lambda_{probe} = 400$ nm) decays mainly with a short component of 25 ns (85%) and a longer one of ~40 μs (15%). We believe that the long lifetime is due to the decomposition of a small amount of the rhenium complex during the measurement resulting in a disruption of the assembly. Using the 25 ns decay (the major component), the rate of the back-electron transfer is calculated to be 4×10^7 s^{-1}. Such a value is in excellent agreement with the rate of the back-electron transfer reported for the covalently linked system $[Re(MQ^+)(CO)_3(dmb)]^{2+}$ (dmb = 4,4′-dimethyl-2,2′-bipyridine; MQ^+ = *N*-methyl-4,4′-bipyridinium), where the methyl viologen is one of the ligands of the rhenium complex. In that case, the lifetime of the CS state was determined to be 26 ns in DCM, corresponding to a rate of 3.9×10^7 s^{-1} for the back-electron transfer.[35]

To have a quantitative analysis of the fast forward electron transfer, femtosecond transient absorption spectroscopy was performed. Excitation in the ^{1}MLCT band of the **G2** component, at 400 nm, was chosen to have a selective population of the rhenium-based component excited state. The formation of the charge-transfer state was probed at 625 nm, which is similar to

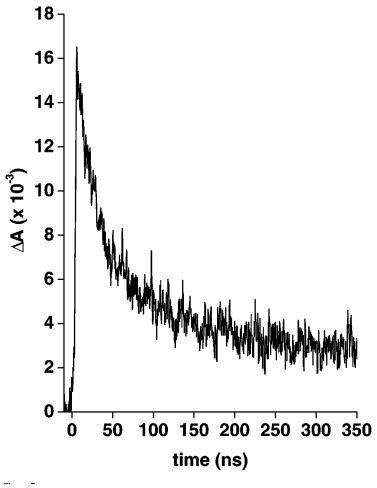

Figure 7. TA trace probed at 400 nm for BAr_f−**H1·G2** (CH_2Cl_2; λ_{exc} = 435 nm).

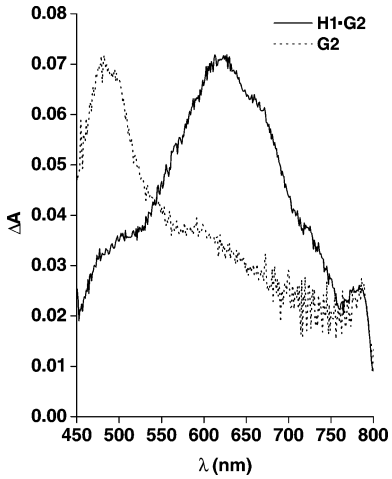

Figure 8. Full TA spectrum of **G2** and of the host−guest complex BAr_f−**H1·G2** recorded 2.5 ps after the laser pulse (CH_2Cl_2; λ_{exc} = 400 nm).

one of the maxima of the absorption of the reduced methyl viologen. Figure 8 shows the full TA spectra in DCM of **G2** and the host−guest complex BAr_f−**H1·G2** 2.5 ps after the laser pulse (λ_{exc} = 400 nm).

A significant part (57%) of the 625-nm transient is formed instantaneously, i.e., within the instrument time resolution ($k_{fet,1} > 7 \times 10^{12}$ s^{-1}) (Figure 9). A slower increase then ensues, of which the kinetics fit the equation $\Delta A = A_0' + A_1'(1 - \exp(-t/\tau_r))$, with a rise time of τ_r = 400 fs (43%), indicating that the rate of the forward electron transfer ($k_{fet,2}$) is 2.5×10^{12} s^{-1} (lower limit) (see Figure 9). No other processes concerning the formation of CS states are observed in this time scale. In view of these experimental results, we believe that the formation of the CS state occurs via two different processes.

Excitation at 400 nm leads to the population of the **G2** ^{1}MLCT state that can undergo intersystem crossing to the lower-lying triplet state or directly to the CS state. Very recently, it was reported that ultrafast photoinduced processes could occur from the singlet excited state of transition-metal complexes.[65] If the process would occur from the singlet excited state, an extremely fast rate constant is expected, based on a larger ΔG value (see Figure 6), which competes with the population of the ^{3}MLCT state. The second "slower" process is a stepwise mechanism, leading first to the population of the ^{3}MLCT state

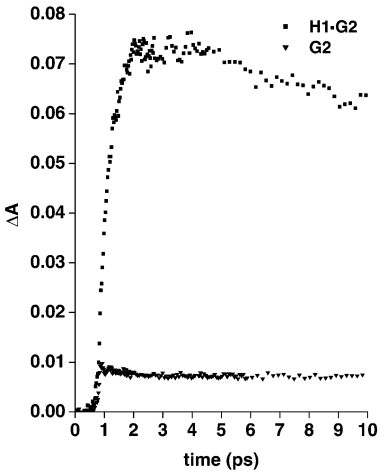

Figure 9. TA trace probed at 625 nm for **G2** and BAr_f−**H1·G2** (CH_2Cl_2; λ_{exc} = 400 nm), showing, on one hand, the formation of the ^{3}MLCT excited state in the case of **G2** and, on the other hand, the formation of the CS state in the case of BAr_f−**H1·G2**.

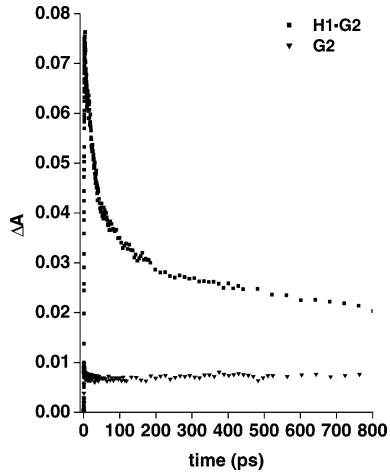

Figure 10. TA trace probed at 625 nm, showing the decay of the TA signal on a subnanosecond time scale (0−800 ps) for **G2** and BAr_f−**H1·G2** (CH_2Cl_2; λ_{exc} = 400 nm).

and then to the electron transfer, via the receptor, also resulting in the formation of the CS state. Another possible interpretation of the data, to explain the two different rates, is related to the "arrangement" of the adduct. We believe that two different conformations of BAr_f−**H1·G2** in solution are possible: one in which the methyl viologen unit is in very close proximity to **G2**, and one in which the methyl viologen unit points away from **G2**. In the first case, the electron transfer is expected to be extremely fast, because the electron donor and the electron acceptor are almost in contact with each other. The role that the hydrogen bonds have then would be negligible, because the electron-transfer process would not involve the connector but would proceed through space. In such a case, a through-solvent tunneling mechanism may provide a reasonable explanation for the ultrafast kinetics. In the fully stretched conformation, on the other hand, the donor and acceptor moieties are far from each other (see Scheme 1), the process is expected to be slower and the role that the six hydrogen bonds have becomes relevant. However, it is remarkable to realize how fast the photoinduced process is in such hydrogen-bonded systems. The rates observed for the self-assembled systems are, in fact, comparable of those reported for the covalently linked system, $[Re(MQ^+)(CO)_3(dmb)]^{2+}$.

The formation of the CS state is also followed by a multiexponential decay to the ground state. In the picosecond time domain, the lifetime decreases with a component of 29 ps, whereas a significant portion does not decay on that time scale (Figure 10).

Also, in this case, the CS states of the two conformers are expected to decay with different rates related to the geometrical arrangement of the assemblies. The long decay, which, according to this trace, is ~50%, is in agreement with the decay (25 ns) of the CS state in the nanosecond TA spectrum (see Figure 5a and 5b) and it is also associated with the slower electron-transfer process. Note that the back-electron transfer rates are, in any case, orders of magnitude slower than the forward processes. These results can be explained on the basis of the Marcus inverted region, because the process in this case is extremely exoergonic ($\Delta G = -1.67$ eV) (see Figure 6).

Conclusions

This paper reports a hydrogen-bonded donor−acceptor dyad that consists of a rhenium complex and a viologen derivative. The components show luminescence and (transient) absorption properties that are dramatically changed when self-assembly of the complementary species occurs in apolar solvents. The resulting complex shows that an ultrafast photoinduced electron transfer occurs from the excited rhenium complex (electron donor) to the viologen-host molecule (electron acceptor). The kinetics of the electron transfer in the hydrogen-bonded system, BAr_f−**H1·G2**, are similar to the electron-transfer kinetics reported for the covalently linked system, $[Re(MQ^+)(CO)_3(dmb)]^{2+}$. This emphasizes that the introduction of a reversible connection between the electron donor and the electron acceptor does not necessarily result in slower kinetics of the electron-transfer processes, as compared to the corresponding covalently linked system. Since the forward electron transfer is 4 orders of magnitude faster than the charge recombination, this type of self-assembled system can be an interesting building block in the design of large structures exhibiting long-range electron-transfer processes. The supramolecular approach offers the possibility to create libraries of donor−acceptor couples to search for the most-efficient combinations and enables the synthesis of such structures.

Acknowledgment. The authors thank Prof. Dr. F. Vögtle (University of Bonn) for inspiring this work, Jan-Meine Ernsting for his assistance with the DOSY experiments, Michael Zimine for measuring the kinetics on the femtosecond setup, and Frank Greydanus and Martijn van Kesteren for their contribution to the synthesis. Han Peeters is kindly acknowledged for measuring the HR−FAB mass spectra. This work was financially supported by NWO-CW.

References and Notes

(1) Lawrence, D. S.; Jiang, T.; Levett, M. *Chem. Rev.* **1995**, *95*, 2229.
(2) Lehn, J.-M. *Science* **2002**, *295*, 2400.
(3) Reinhoudt, D. N.; Crego-Calama, M. *Science* **2002**, *295*, 2403.
(4) Lehn, J.-M. *Supramolecular Chemistry*; Wiley−VCH Verlag GmbH: Weinheim, Germany, 1995.
(5) Fujita, M., Ed. *Molecular Self-Assembly. Organic versus Inorganic Approaches*; Structure and Bonding Vol. 96; Springer−Verlag: Berlin, Germany, 2001.
(6) Ward, M. D.; Barigelletti, F. *Coord. Chem. Rev.* **2001**, *216−217*, 127. (b) Ward, M. D. *Chem. Soc. Rev.* **1997**, *26*, 365.
(7) Pol, Y. V.; Suau, R.; Perez-Inestrosa, E.; Bassani, D. M. *Photochem., Photobiol. Sci.* **2003**, *2*, 1152. (b) McClenaghan, N. D.; Absalon, C.; Bassani, D. M. *J. Am. Chem. Soc.* **2003**, *125*, 13004. (c) McClenaghan, N. D.; Absalon, C.; Bassani, D. M. *Chem. Commun.* **2004**, 1270.
(8) Hayashi, T.; Ogoshi, H. *Chem. Soc. Rev.* **1997**, *26*, 355.
(9) Reinhoudt, D. N., Ed. *Comprehensive Supramolecular Chemistry*; Pergamon Press: Oxford, England, 1996; Vol. 10. (b) Atwood, J. L., Davies, J. E. D., MacNicol, D. D., Vögtle, F., Eds. *Comprehensive Supramolecular Chemistry*; Pergamon/Elsevier: Oxford, U.K., 1996.
(10) Balzani, V.; Credi, A.; Venturi, M. *Molecular Devices and Machines. A Journey into the Nano World*; Wiley−VCH: Weinheim, Germany, 2003.
(11) Beer, P. D.; Gale, P. A. *Angew. Chem., Int. Ed.* **2001**, *40*, 486. (b) Uppadine, L. H.; Keene, F. R.; Beer, P. D. *J. Chem. Soc., Dalton Trans.* **2001**, 2188. (c) Cooper, J. B.; Drew, M. G. B.; Beer, P. D. *J. Chem. Soc., Dalton Trans.* **2001**, 392. (d) Beer, P. D. *Acc. Chem. Res.* **1998**, *31*, 71.
(12) Cary, D. R.; Zaitseva, N. P.; Gray, K.; O'Day, K. E.; Darrow, C. B.; Lane, S. M.; Peyser, T. A.; Satcher, J. H., Jr.; Van Antwerp, W. P.; Nelson, A. J.; Reynolds, J. G. *Inorg. Chem.* **2002**, *41*, 1662.
(13) de Silva, A. P.; Gunaratne, H. Q. N.; Gunnlaugsson, T.; Huxley, A. J. M.; McCoy, C. P.; Rademacher, J. T.; Rice, T. E. *Chem. Rev.* **1997**, *97*, 1515.
(14) Czarnik, A. W. *Acc. Chem. Res.* **1994**, *27*, 302.
(15) James, T. D.; Sandanayake, K. R. A. S.; Shinkai, S. *Angew. Chem., Int. Ed. Engl.* **1994**, *33*, 2207.
(16) Hoeben, F. J. M.; Herz, L. M.; Daniel, C.; Jonkheijm, P.; Schenning, A. P. H. J.; Silva, C.; Meskers, S. C. J.; Beljonne, D.; Phillips, R. T.; Friend, R. H.; Meijer, E. W. *Angew. Chem., Int. Ed.* **2004**, *43*, 1976.
(17) Chang, C. J.; Brown, J. D. K.; Chang, M. C. Y.; Baker, E. A.; Nocera, D. G. In *Electron Transfer in Chemistry*; Balzani, V., Ed.; Wiley−VCH Verlag GmbH: Weinheim, Germany, 2001; Vol. 3, p 409.
(18) Balzani, V., Scandola, F., Eds. *Supramolecular Chemistry*; Horwood: Chichester, England, 1991.
(19) Hamilton, A. D. In *Advances in Supramolecular Chemistry*; Gokel, G. W., Ed.; JAI Press, Ltd.: London, 1990; p 1.
(20) Balzani, V.; Scandola, F. In *Comprehensive Supramolecular Chemistry*; Pergamon Press: Oxford, England, 1996; Vol. 10, p 687.
(21) Guldi, D. M. *Chem. Soc. Rev.* **2002**, *31*, 22.
(22) Ahrens, M. J.; Sinks, L. E.; Rybtchinski, B.; Liu, W.; Jones, B. A.; Giaimo, J. M.; Gusev, A. V.; Goshe, A. J.; Tiede, D. M.; Wasielewski, M. R. *J. Am. Chem. Soc.* **2004**, *126*, 8284.
(23) Smitha, M. A.; Prasad, E.; Gopidas, K. R. *J. Am. Chem. Soc.* **2001**, *123*, 1159.
(24) Sessler, J. L.; Wang, B.; Harriman, A. *J. Am. Chem. Soc.* **1993**, *115*, 10418.
(25) Sessler, J. L.; Brown, C. T.; O'Connor, D.; Springs, S. L.; Wang, R.; Sathiosatham, M.; Hirose, T. *J. Org. Chem.* **1998**, *63*, 7370.
(26) Sessler, J. L.; Sathiosatham, M.; Brown, C. T.; Rhodes, T. A.; Wiederrecht, G. *J. Am. Chem. Soc.* **2001**, *123*, 3655.
(27) Ghaddar, T. H.; Castner, E. W.; Isied, S. S. *J. Am. Chem. Soc.* **2000**, *122*, 1233.
(28) Würthner, F.; Chen, Z.; Houben, F.; Osswald, P.; You, C.-C.; Jonkheijm, P.; van Herrikhuyzen, J.; Schenning, A. P. H. J.; van der Schoot, P. P. A. M.; Meijer, E. W.; Beckers, E. H. A.; Meskers, S. C. J.; Janssen, R. A. J. *J. Am. Chem. Soc.* **2004**, *126*, 10611.
(29) Osuka, A.; Yoneshima, R.; Shiratori, H.; Okada, T.; Tanigushi, S.; Mataga, N. *Chem. Commun.* **1998**, 1567.
(30) Deng, Y. Q.; Roberts, J. A.; Peng, S. -M.; Chang, S. K.; Nocera, D. G. *Angew. Chem., Int. Ed. Engl.* **1997**, *36*, 2124.
(31) Kirby, J. P.; Roberts, J. A.; Nocera, D. G. *J. Am. Chem. Soc.* **1997**, *119*, 9230.
(32) Piotrowiak, P. *Chem. Soc. Rev.* **1999**, *28*, 143.
(33) Chang, S.-K.; Hamilton, A. D. *J. Am. Chem. Soc.* **1988**, *110*, 1318.
(34) Salameh, A. S.; Ghaddar, T.; Isied, S. S. *J. Phys. Org. Chem.* **1999**, *12*, 247.
(35) Liard, D. J.; Vlèek, A., Jr. *Inorg. Chem.* **2000**, *39*, 485.
(36) Liard, D. J.; Kleverlaan, C. J.; Vlèek, A., Jr. *Inorg. Chem.* **2003**, *42*, 7995.
(37) Liard, D. J.; Busby, M.; Farrell, I. R.; Matousek, P.; Towrie, M.; Vlèek, A., Jr. *J. Phys. Chem. A* **2004**, *108*, 556. (b) The Gibbs free energy change for the electron-transfer process (ΔG_{el}) is given by $\Delta G_{el} = e(E_{ox}(D) - E_{red}(A)) - E_{00}$. The reduction potential of the viologen and the oxidation potential of the rhenium complex are, respectively, −0.45 V and +1.32 V.
(38) Ashton, P. R.; Ballardini, R.; Balzani, V.; Credi, A.; Dress, K. R.; Ishow, E.; Kleverlaan, C. J.; Kocian, O.; Preece, J. A.; Spencer, N.; Stoddart, J. F.; Venturi, M.; Wenger, S. *Chem.−Eur. J.* **2000**, *6*, 3558.
(39) Scandola, F.; Chiorboli, C.; Indelli, M. T.; Rampi, M. A. In *Electron Transfer in Chemistry*; Balzani, V., Ed.; Wiley−VCH Verlag GmbH: Weinheim, Germany, 2001; Vol. 3, p 337.
(40) De Cola, L.; Belser, P. *Coord. Chem. Rev.* **1998**, *177*, 301.
(41) Barigelletti, F.; Flamigni, L. *Chem. Soc. Rev.* **2000**, *29*, 1.
(42) Kleverlaan, C. J.; Indelli, M. T.; Bignozzi, C. A.; Pavanin, L.; Scandola, F.; Hasselman, G. M.; Meyer, G. J. *J. Am. Chem. Soc.* **2000**, *122*, 2840.

(43) Yonemoto, E. H.; Saupe, G. B.; Schmehl, R. H.; Hubig, S. M.; Riley, R. L.; Iverson, B. L.; Mallouk, T. E. *J. Am. Chem. Soc.* **1994**, *116*, 4786.

(44) Stufkens, D. J.; Vlèek, A., Jr. *Coord. Chem. Rev.* **1998**, *177*, 127.

(45) Ashton, P. R.; Balzani, V.; Credi, A.; Kocian, O.; Prodi, L.; Spencer, N.; Stoddart, J. F. *J. Am. Chem. Soc.* **1998**, *120*, 11190.

(46) Ashton, P. R.; Balzani, V.; Credi, A.; Kocian, O.; Pasini, D.; Prodi, L.; Spencer, N.; Stoddart, J. F.; Tolley, M. S.; Venturi, M.; White, A. J. P.; Williams, D. J. *Chem.—Eur. J.* **1998**, *4*, 590.

(47) Vlèek, A., Jr.; Farrell, I. R.; Liard, D. J.; Matonsek, P.; Towrie, M.; Parker, A. W.; Grills, D. C.; George, M. W. *J. Chem. Soc., Dalton Trans.* **2002**, 701.

(48) Chen, P.; Duesing, R.; Graff, D. K.; Meyer, T. J. *J. Phys. Chem.* **1991**, *95*, 5850.

(49) Schanze, K. S.; MacQueen, D. B.; Perkins, T. A.; Cabana, L. A. *Coord. Chem. Rev.* **1993**, *122*, 63.

(50) Evans, C.-L.; Morris, G. A. Unpublished results.

(51) Vergeer, F.; Kleverlaan, C. J.; Stufkens, D. J. *Inorg. Chim. Acta* **2002**, *327*, 126.

(52) Kelly, L. A.; Rodgers, M. A. J. *J. Phys. Chem.* **1994**, *98*, 6386.

(53) Tecilla, P.; Dixon, R. P.; Slobodkin, G.; Alavi, D. S.; Waldeck, D. H.; Hamilton, A. D. *J. Am. Chem. Soc.* **1990**, *112*, 9408.

(54) Chang, S.-K.; Van Engen, D.; Fan, E.; Hamilton, A. D. *J. Am. Chem. Soc.* **1991**, *113*, 7640.

(55) Dirksen, A.; Hahn, U.; Schwanke, F.; Nieger, M.; Reek, J. N. H.; Vögtle, F.; De Cola, L. *Chem.—Eur. J.* **2004**, *10*, 2036.

(56) Reger, D. L.; Wright, T. D.; Little, C. A.; Lamba, J. J. S.; Smith, M. D. *Inorg. Chem.* **2001**, *40*, 3810.

(57) Chin, T.; Gao, Z.; Lelouche, I.; Shin, Y. K.; Purandare, A.; Knapp, S.; Isied, S. S. *J. Am. Chem. Soc.* **1997**, *119*, 12849.

(58) Rossenaar, B. D.; Stufkens, D. J.; Vlèek, A., Jr. *Inorg. Chem.* **1996**, *33*, 2902.

(59) Johnson, C. S., Jr. *Prog. Nucl. Magn. Reson. Spectrosc.* **1999**, *34*, 203.

(60) Gounarides, J. S.; Chen, A.; Shapiro, M. J. *J. Chromatogr. B* **1999**, *725*, 79.

(61) Stejskal−Tanner equation: $\ln(I/I_0) = -[\gamma^2\delta^2G^2(\Delta - \delta/3)]D$, where I is the peak area, I_0 the peak area in the absence of gradients, γ the magnetogyric ratio of the observed nucleus, δ the gradient duration, G the strength of the gradient pulse in T/m, Δ the diffusion time, and D the diffusion coefficient.

(62) Stejskal, E. O.; Tanner, J. E. *J. Chem. Phys.* **1965**, *42*, 288.

(63) The Stokes−Einstein equation: $D = (k_BT)/(6\pi\eta r)$, where D is the diffusion coefficient, k_B the Boltzmann constant, T the absolute temperature (in degrees Kelvin), η the viscosity of the solution, and r the radius of the molecular sphere. The viscosity of neat acetonitrile-d_3 was used: η (22 °C) = 0.36 ± 0.02 cP.

(64) Watanabe, T.; Honda, K. *J. Phys. Chem.* **1982**, *86*, 2617.

(65) Andersson, J.; Puntoriero, F.; Serroni, S.; Yartsev, A.; Pascher, T.; Polívka, T.; Campagna, S.; Sundström, V. *Chem. Phys. Lett.* **2004**, *386*, 336.